PAPER

NJC
www.rsc.org/njc

Bent and planar molecules in polymorphs of the tricyclic carbon sulfide C_6S_8

Johannes Beck,*[a] Johannes Weber,*[b] Atashi Basu Mukhopadhyay[b] and Michael Dolg[b]

[a] *Institute for Inorganic Chemistry, University of Bonn, Gerhard-Domagk-Str. 1, D-53121 Bonn, Germany. E-mail: j.beck@uni-bonn.de; Fax: +49-228-735660*

[b] *Institute for Theoretical Chemistry, University of Cologne, Greinstr. 4, D-50939 Cologne, Germany. E-mail: Johannes.Weber@uni-koeln.de; Fax: +49-221-470-6896*

Received (in Montpellier, France) 24th February 2004, Accepted 14th October 2004
First published as an Advance Article on the web 26th January 2005

The binary sulfur-carbon compound C_6S_8 (3*H*,7*H*-bis[1,2]dithiolo[3,4-b:3′,4′-e][1,4]dithiine-3,7-dithione) was synthesized and characterized in 1993 by Rauchfuss *et al.* The crystal structure determination (monoclinic, space group $P2_1/c$) revealed an essentially planar molecular shape (α-C_6S_8). Repeating the synthetic procedure of Rauchfuss we obtained red crystals of C_6S_8 in a second crystallographic form (β-C_6S_8, tetragonal, space group $P\bar{4}2_1c$). Additionally, the formation of a black, insoluble, amorphous sulfur-carbon polymer with the tentative formula $(C_6S_8)_n$ was observed. The molecules in β-C_6S_8 are angled along the S–S axis of the central 1,4-dithiine ring. The dihedral angle between the two planar C_3S_5 moieties is 133°. The molecular geometry, IR, Raman and UV spectra of C_6S_8 are analyzed theoretically at the B3LYP/cc-pVTZ level and are compared with experimental data. Assignments of vibrations and electronic transitions are made. A C_2 symmetric, bent molecular structure is found for C_6S_8, in agreement with the crystal structure of the β-form, which is only a few kJ mol^{-1} more stable than the planar structure found in the α-C_6S_8 polymorph. C_6S_8 is a rare example of a substituted 1,4-dithiine that is structurally characterized in both the planar and bent forms.

Introduction

Sulfur and carbon form a series of molecular crystalline and of polymeric, mainly amorphous, binary compounds. Rauchfuss and coworkers described in 1993 the synthesis (see Scheme 1) of a novel carbon sulfide C_6S_8 (**1**) by dimerization of the dithiole β-$H_2C_3S_5$ with elimination of H_2S.[1] A crystallographic study revealed an essentially planar molecular shape for the tricyclic molecule, which we refer to as the α-form. In the course of our studies on the poorly characterized amorphous, polymeric carbon sulfides we focused our interest on this reaction, since we observed that besides the soluble molecular form of C_6S_8, a black, insoluble, amorphous material of approximately the same composition is formed. When identifying the red soluble material by means of crystallography, surprisingly a second polymorph of C_6S_8, with a different unit cell and crystal system and different molecular shape than already described for **1**, was found. We call the second polymorph β-C_6S_8 in the following. Here we describe its crystal structure, its vibrational and UV/Vis spectra as well as a theoretical investigation to understand the significant differences in the molecular shapes present in α- and β-C_6S_8.

A look in the literature reveals that similar polymorphism has been reported for some other molecules composed of sulfur and carbon, too.[2–5] Especially interesting in connection with this publication is the work of Mastryukov *et al.*[4] who theoretically investigated the planarity and non-planarity of thianthrene-like molecules in molecular mechanics (MM3) and *ab initio* (HF/3-21G*) studies. Thianthrenes as well as the title compound possess the same central 1,4-dithiine ring as a structural unit and we will show in the following that the floppiness of this unit can be regarded as the origin of the unexpected polymorphism.

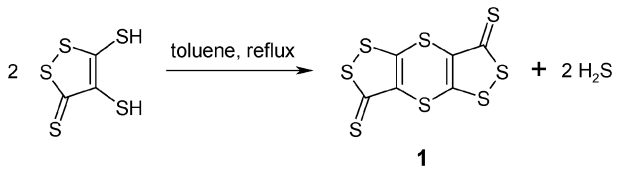

1

Scheme 1 The conversion of β-$H_2C_3S_5$ into C_6S_8 (**1**) as described by Rauchfuss *et al.*[1]

Experimental

Synthesis and NMR spectrum

β-$H_2C_3S_5$ was prepared by the method of Steimecke *et al.*[6] C_6S_8 was obtained by the procedure described by Rauchfuss *et al.* by heating β-$H_2C_3S_5$ in toluene under a flow of Ar.[1] After 24 h of reflux the reaction mixture consisted of a red-colored solution and a dark insoluble material. The mixture was filtered while hot. On cooling the filtrate C_6S_8 formed as a red precipitation. The raw material was recrystallized twice by slow diffusion of hexane into a saturated solution of C_6S_8 in THF, leading to red needle-shaped crystals. Mp 255 °C; anal. calcd for C_6S_8 22.0 C, 78.0 S; found 22.4 C, 76.4 S.

Initially, we were not able to obtain a ^{13}C NMR spectrum of **1**. Despite the saturated solution having a light-red coloration the concentration was too low to obtain substantial intensities in the NMR experiment. This is in agreement with the observation of Rauchfuss *et al.*[1] So we prepared a ^{13}C enriched sample. The synthesis of β-$H_2C_3S_5$ was repeated starting from $^{13}CS_2$ in a concentration to achieve a ^{13}C enrichment of 15%. The sample of C_6S_8 prepared by this way showed the expected number of three resonances at 132.7, 165.1 and 202.5 ppm, which can be attributed to the resonances of the three distinct carbon nuclei C(1), C(2) and C(3) present in **1** (see Fig. 1).

DOI: 10.1039/b402881c

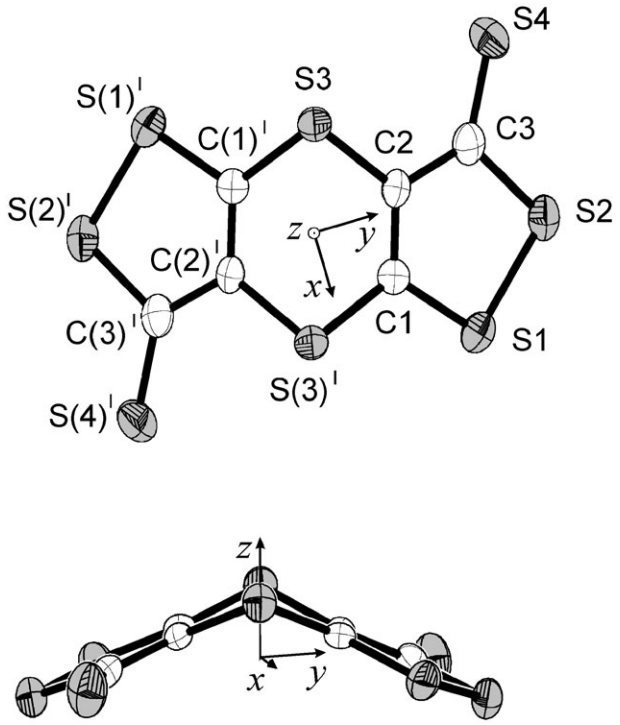

Fig. 1 The C_6S_8 molecule in the crystal structure of β-C_6S_8 in a view along the twofold axis (top) and along the S(3)–S(3^1) axis (bottom). Thermal ellipsoids are scaled to enclose a probability density of 50%. Symmetry operator: $I = 1 - x, 2 - y, z$. The cartesian coordinate system at the molecule's center-of-mass denotes the placement of the molecule in the quantum chemical calculations.

Crystal structure analysis

A needle-shaped crystal of dimensions 0.03 × 0.03 × 0.88 mm^3 was selected for the single crystal diffraction study. Precession photographs showed the tetragonal lattice. Intensity data were recorded using an Enraf-Nonius CAD4 diffractometer and graphite monochromated Cu-Kα radiation. Examination of the reciprocal lattice revealed the Laue class 4/*mmm*. Data averaging in this class led to $R_{int} = 0.053$. The absence of integral extinctions, the presence of zonal extinctions (*hhl*: $l = 2n$), and serial extinctions (*h*00: $h = 2n$; 0*k*0: $k = 2n$; *00l*: $l = 2n$) led to the acentric space group $P\bar{4}2_1c$. Crystal data: C_6S_8, $M = 1458.5$, $a = b = 11.9524(8)$, $c = 7.6116(4)$ Å, $U = 1087.4$ Å^3, $T = 295$ K, $Z = 4$, μ(Cu-Kα) = 14.8 mm^{-1}, 2973 reflections measured in the range $4° < 2\theta < 110°$, 681 unique that were used in all fits. A structure model was obtained by direct methods[7] and refined by full-matrix least squares based on F^2 with anisotropic displacement parameters for all atoms.[8] The final $wR(F^2)$ was 0.085 (all data) and $R(|F|) = 0.035$ for 571 reflections with $I > 2\sigma(I)$. The maximal and minimal residual electron density was +0.25/−0.42 e/10^6 pm^3. The Flack parameter of 0.04(8) was essentially zero within the standard deviation, indicating the correct polarity for the structure model.†

IR, Raman and UV spectra

IR spectra were recorded at ambient temperature from a KBr pellet in the spectral range 4000–500 cm^{-1} and from a CsI pellet in the range 600–200 cm^{-1} with a Bruker IFS 113v spectrometer. Raman spectra were measured from a crystalline sample in a thin-walled glass capillary at ambient temperature on a Bruker RFS100 spectrometer. An UV/Vis spectrum of C_6S_8 was recorded on a Gröbel diode array spectrometer in $CHCl_3$ solution.

Computational details

The molecular geometry, normal modes, IR and Raman intensities of **1** were computed quantum chemically from first principles by using Hartree–Fock (HF) and density functional methods (DFT) employing the BP86,[9] BLYP[10] and B3LYP[11] functionals. For the assignment of the UV/Vis spectrum vertical excitation energies and transition dipole moments were calculated within the TD-DFT formalism.[12] All calculations mentioned so far were done with the Gaussian98 package.[13] To obtain accurate relative energies between different conformers, MP2 and CCSD calculations were performed at several geometries using the Molpro package.[14] The conventional choice for the coordinate system was made (see Fig. 1 below), where the C_2 symmetry axis coincides with the z axis. Effects of the limited basis set were investigated by employing different atomic basis sets, namely 3-21 + G*,[15] cc-pVDZ,[16] TZVP(P)[17] and cc-pVTZ.[16] For some calculations the cc-pVQZ[11] set was used and the cc sets were augmented with diffuse functions.[18] All method/basis set combinations gave qualitatively the same results. In the following discussion, we focus on the calculations with the hybrid B3LYP method in combination with the cc-pVTZ basis set for all atoms. For a better comparison of experimental IR, Raman and UV spectra with the theoretical results, the line spectra obtained from Gaussian98 were folded with a Lorentzian lineshape function with an empirical broadening using the program LineShaper.[19] All 3D rendered visualizations were done with Molekel.[20] The counterpoise (CP) correction[21,22] was employed to obtain molecular interaction energies corrected for the basis set superposition error (BSSE), which was calculated with the Turbomole program[23] at the RI-MP2 level.[24] In the RI-MP2 method a significant acceleration of the calculation compared to the usual MP2 method is achieved by approximating products of atomic orbitals (AO), $\mu(r)\nu(r) = \rho_{\mu\nu}(r)$, occurring in two-electron, four-center integrals by a linear combination of atom-centered auxiliary basis functions, $\rho_{\mu\nu}(r) \approx \Sigma_P\, c_{\mu\nu P}\, P(r)$. In the Turbomole RI-MP2 implementation the energy contribution of the four-center integrals is obtained by applying this approximation twice:[25]

$$(\mu\nu|\kappa\lambda) \approx \sum_{P,Q} (\mu\nu|P)(P|Q)^{-1}(Q|\kappa\lambda) \qquad (1)$$

If the auxiliary basis $\{P\}$ was complete and orthonormal the expansion on the right-hand side of eqn. (1) would be an insertion of the *resolution of identity* [RI, $I = \Sigma_P|P)(P|$] two times and would be exact. In order to reduce the computational effort, on the one hand the size of the auxiliary basis $\{P\}$ has to be significantly smaller than the square of the size of the AO basis. On the other hand, a sufficiently large auxiliary basis is necessary to keep numerical inaccuracies small. We used high-quality auxiliary basis sets that have been designed specially for the reference AO basis sets (cc-pVDZ, cc-pVTZ, cc-pVQZ, aug-cc-pVTZ and aug-cc-pVQZ) and the quantum chemical model (MP2).[25] The auxiliary basis corresponding to the most extended AO set (aug-cc-pVQZ) is composed of uncontracted 12 s, 10 p, 9 d ,7 f, 4 g and 2 h functions on each sulfur atom and 9 s, 8 p, 7 d, 6 f, 4 g, and 2 h functions on each carbon atom. The loss in accuracy turns out to be negligible (<0.5 kJ mol^{-1} in our calculations) compared to other approximations (limited AO sets, post-HF model) that are made in the course of the calculations.

† CCDC reference number 255756. See http://www.rsc.org/suppdata/nj/b4/b402881c/ for crystallographic data in .cif or other electronic format.

Results and discussion

Crystal and molecular structure of β-C_6S_8 in comparison with the α-form

The tetragonal unit cell of β-C_6S_8 contains 4 molecules. An individual molecule is shown in Fig. 1. A twofold axis runs through the center of the central C_4S_2 ring, giving the molecule crystallographic C_2 symmetry. The two C_3S_5 moieties are essentially planar with the largest deviation of an atom from the best least-squares plane being 0.03 Å. The two planar moieties are folded at the S(3)–S(3^I) axis with an interplanar angle of 133°.

Since the molecules in the two polymorphs are of different shapes the relation between the two forms can be called conformational polymorphism.[26] A unique observation made in our laboratory is the fact that we could not obtain crystals of the α-form despite several attempts. In all our crystallization experiments only the needle-shaped crystals of the β-polymorph appeared. The use of different solvent mixtures including the one described by Rauchfuss *et al.*[1] was without success. To verify this observation we took powder X-ray diffractograms of the bulk samples. The first precipitates obtained from the hot toluene reaction mixture showed only weak and broadened reflections, indicating poor crystallinity of the material. Powder samples obtained from slowly grown crystals, for example from THF–hexane, gave good quality diffractograms that could be indexed on the basis of the tetragonal unit cell of the β-form. The phenomenon is not uncommon and is known in the literature as "disappearing polymorphs".[27] It is believed that the crystal seed, when once formed from a thermodynamically more favored polymorph, avoids the crystallization of other forms. This idea is underlined by the observation of the reappearance of polymorphs that had disappeared for decades.[28]

With the exception of the significant bending, the bond lengths and angles of the molecule of the β-form are in close agreement to the two independent molecules present in the unit cell of the α-form (Table 1). The bent molecules of the β-form are chiral. There are, however, both enantiomorphs present in the unit cell. The non-centrosymmetry of the space group finds its expression in a polar stacking arrangement of the molecules along the crystallographic *c* axis (Fig. 2 and Fig. 3). In the stack of β-polymorphic molecules the shortest interatomic distance between two molecules is 3.54 Å (C1–C3). The shortest intermolecular distance between atoms of neighboring molecules in parallel running stacks is 3.31 Å (S1–S4). The planar molecules of the α-form are stacked with the shortest intermolecular atomic distance begin 3.47 Å (between carbon atoms). Again, the shortest intermolecular contacts of 3.24 Å are observed between sulfur atoms of neighboring molecules across the stacking direction. At first sight, the smaller distances in the α-form seem to suggest that stronger intermolecular interactions are present in α-C_6S_8. However, evidence will be given below that the polar stacking of β-C_6S_8 increases its stability over the α-form.

Our quantum chemical calculations on the free molecule compare well with the experimental results described above. A bent, C_2-symmetric molecular structure is predicted, too. The moieties are almost planar since the largest atomic displacement from the least squares plane is equal to 0.07 Å. The interplanar angle, which can in good approximation be expressed by the dihedral angle C(1^I)–S(3)–S(3^I)–C(1), is calculated to be 141.7°. Experimental and theoretical geometrical parameters are compared in Table 1. The RMS deviation of bond lengths and bond angles amounts to 0.007 Å or 0.4°, respectively. A larger angular deviation is obtained for the

Table 1 Experimental and theoretical (B3LYP/cc-pVTZ) geometrical parameters (bond lengths in Å, angles in deg.) of β-C_6S_8 (**1**). Atomic labels as in Fig. 1. Numbers in parentheses denote the bond parameters of the planar species, referred to as α-C_6S_8

Parameter	Experiment	Theory
C(1)–S(3^I)	1.746 (1.749)	1.759 (1.756)
C(1)–C(2)	1.343 (1.364)	1.359 (1.360)
C(2)–S(3)	1.764 (1.764)	1.782 (1.783)
C(1)–S(1)	1.735 (1.719)	1.741 (1.747)
C(2)–C(3)	1.442 (1.426)	1.433 (1.431)
C(3)–S(4)	1.636 (1.647)	1.650 (1.653)
C(3)–S(2)	1.741 (1.733)	1.760 (1.756)
S(2)–S(1)	2.064 (2.059)	2.104 (2.100)
C(2)–S(3)–C(1^I)	98.0 (101.9)	100.25 (102.11)
S(3)–C(1^I)–C(2^I)	126.0 (129.7)	127.79 (130.74)
C(1)–C(2)–S(3)	122.8 (128.3)	123.70 (127.16)
C(2)–C(1)–S(1)	118.3 (117.5)	117.88 (117.25)
C(1)–S(1)–S(2)	93.2 (94.2)	93.27 (93.84)
C(3)–S(2)–S(1)	98.0 (97.1)	96.79 (96.40)
S(2)–C(3)–C(2)	111.5 (112.8)	112.19 (112.93)
C(3)–C(2)–C(1)	119.1 (118.4)	119.61 (119.58)
C(2)–C(3)–S(4)	129.8 (125.3)	128.30 (127.14)
C(1)–C(2)–C(3)–S(4)	−179.5 (177.4)	−176.82 (180.00)
S(1)–C(1)–C(2)–S(3)	179.7 (178.2)	179.76 (180.00)
C(1^I)–S(3)–S(3^I)–C(1)	133.0 (180.00)	141.69 (180.00)

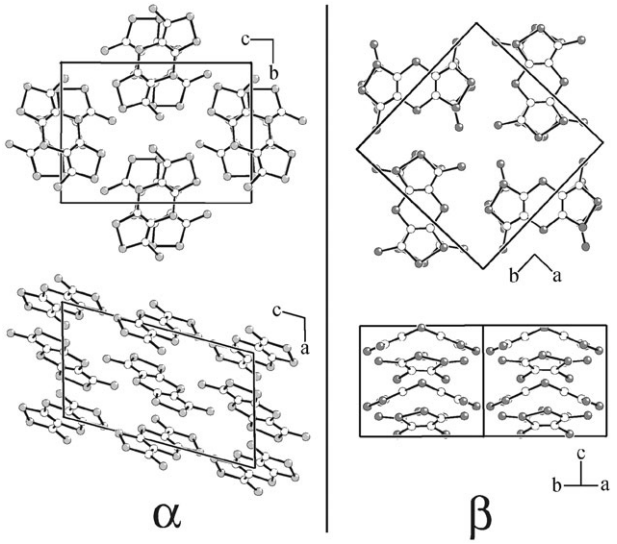

Fig. 2 Crystal structures of the α- (left) and the β-forms (right) of C_6S_8. For both polymorphs two projections are shown, one along the stacking direction of the molecules (top) and one perpendicular to the stacking direction (bottom).

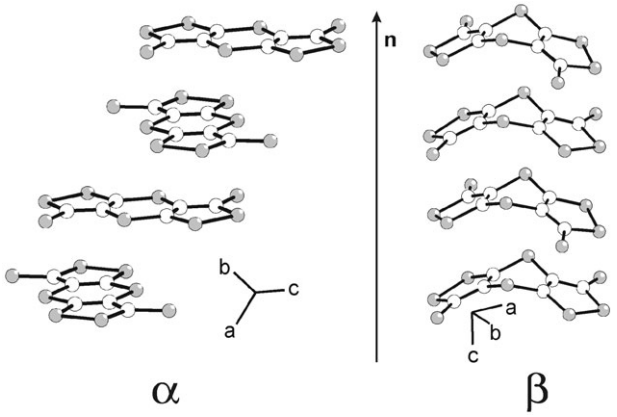

Fig. 3 The stacking arrangement of C_6S_8 molecules in the structures of the α- (left) and the β-form (right). The vector **n** is parallel to the normal vectors of the planes of individual molecules in the α-form and to the crystallographic *c* axis of the β-form.

Table 2 Total energies E, relative energy ΔE of planar C_6S_8 with respect to the bent (β) form, ZPE correction to ΔE and the dihedral angle calculated using different method/basis set combinations

	$E(C_6S_8)$/Hartree				
Method/basis set	Planar	Bent	ΔE/kJ mol^{-1}	ΔZPE[a]/kJ mol^{-1}	C(1^I)–S(3)–S(3^I)–C(1)/deg.
HF/3-21 + G*	−3391.260 091	−3391.261 154	2.8	3.3	128.5
HF/cc-pVTZ	−3407.581 944	−3407.583 909	5.2	−0.7	139.2
BP86/TZVP	−3414.605 325	−3414.607 835	6.6	−1.0	135.3
BP86/TZVPP	−3414.671 497	−3414.672 456	2.5	−0.3	143.0
BLYP/cc-pVTZ	−3414.291 274	−3414.292 665	3.7	−0.4	141.5
B3LYP/TZVPP	−3414.423 064	−3414.424 402	3.5	−0.5	141.7
B3LYP/cc-pVTZ	−3414.472 631	−3414.473 915	3.4	−0.5	141.7
MP2/cc-pVTZ[b]	−3409.594 752	3409.598 057	8.7	—	—
CCSD/cc-pVTZ[b]	−3409.635 395	−3409.638 477	8.1	—	—

[a] Single imaginary frequency of the planar form ignored. [b] Single point calculation at B3LYP/TZVPP geometry.

interplanar angle C(1^I)–S(3)–S(3^I)–C(1), however. Moreover, depending on the theoretical method and the used basis set, variations of this angle over more than 10° were observed (see Table 2).

The high sensitivity obviously results from a very flat potential along the internal motion that turns the bent molecule into a planar one. This is reflected by the lowest frequency mode ν_{19} ("butterfly mode", see Fig. 6 and Table 2), which has a frequency of only 30 cm^{-1}. We also optimized the geometry of C_6S_8 with constrained planar C_{2h} symmetry. The resulting structure is not a minimum on the potential energy surface (PES) but a first-order saddle point (see Fig. 4). At the B3LYP/cc-pVTZ level the energy gap between the bent and the planar species amounts to 3.4 kJ mol^{-1}. Taking into account the zero point energy (ZPE) correction the energy gap decreases further to 2.9 kJ mol^{-1}. As mentioned earlier, the gap varies somewhat depending on the employed theoretical method (RHF, DFT, MP2, CCSD, see Table 2) but using double- and triple-zeta basis sets with additional polarization functions it does not exceed 9 kJ mol^{-1}. In view of this small energy gap, it is probable that in the free molecule the transition state is accessible at room temperature. Hence, a transformation into the other enantiomer should be possible.

Packing effects of the crystal were estimated by HF and RI-MP2 calculations on C_6S_8 dimers in all different relative orientations that can be found for nearest neighbors in the monoclinic α- as well as in the tetragonal β-C_6S_8 crystal structure. The RI-MP2 calculations show that the major part of the complexation energy results from dispersion interactions (at the HF level the interactions are repulsive in most cases), which reach a maximum for pairs of molecules with stacked alignment (*i.e.*, pairs of neighboring molecules that are connected by the normal vectors **n** of the approximate molecular planes). In stacked, planar molecules one usually assumes that the major part of the interaction results from specific π-π interactions, but this is not the case in α-C_6S_8. Here, two types of stacks are present with the **n**-vectors of the constituent molecules being roughly in the directions $\mathbf{n} = a + 0.4 \cdot b$ and $\mathbf{n} = a - 0.4 \cdot b$, respectively. A look along **n** reveals that the stacked neighbours are rotated by approximately 65° to each other. Additionally, the molecules are shifted against each other, as depicted in Fig. 3, so that no specific π-π interaction is present. Rather, n-π and n-n interactions of the sulfur atoms seem to have a dominant effect on the crystal arrangement. In β-C_6S_8 the molecules are stacked along the *c* axis. They form ABA layers, where each layer contains one of the two enantiomers of β-C_6S_8. The parallel orientation of the long molecular axes allows n-n, n-π as well as π-π interactions between the layers (see Fig. 3). The calculated complexation energy of stacked β- and α-C_6S_8 dimers at the RI-MP2/aug-cc-pVQZ level amounts to −128 and −120 kJ mol^{-1}, respectively.‡ Detailed results will be reported elsewhere.[29] Hence, despite the smaller intermolecular distance in the α-form, the bonding forces seem to be stronger between the molecules having the β-form.

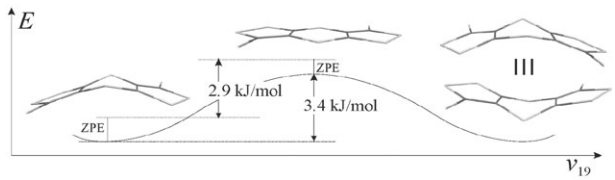

Fig. 4 Schematic potential curve showing the transition between the two enantiomers of β-C_6S_8 *via* the planar structure.

Our results reconfirm the known structural feature of substituted 1,4-dithiacyclohexadienes (the middle ring of C_6S_8), which can, in principle, occur as planar or as bent molecules. For the parent compound **2** we obtained a bent structure with C(1^I)–S(3)–S(3^I)–C(1) = 137.1° at the B3LYP/cc-pVTZ level and a barrier to planarity of 10.3 kJ mol^{-1} (Scheme 2), which is in line with earlier theoretical investigations[30] and the fact that **2** has a bent molecular shape in the crystalline state.[31]

A slight increase or decrease of the barrier caused by substituents, intermolecular interactions or changes in the electronic state is sufficient to change the molecular structure over a wide range. For example, thianthrene is a folded molecule in the crystalline state (interplanar angle between the two phenyl rings = 128°)[32] and in the gas phase (131°).[33] One-electron oxidation yields the radical cation (thianthrene)$^{\bullet+}$ with an almost planar structure (174°).[34] A search in the Cambridge Crystallographic Database (CSD version 5.25, Nov 2003 + 2 updates Jan 2004) for substituted 1,4-dithiines revealed 66 hits with available 3D data of which 38 are bent and 21 planar.[35] For the species we regard as planar the absolute value of the CSSC dihedral angle lies within 180 ± 2°. Seven molecules could not be assigned unequivocally since they possess a small deviation from planarity in the range of 3–13°. A histogram of the distribution of CSSC dihedral angles is shown in Fig. 5. Most of the bent species exhibit a dihedral angle between 122° and 138°.

Vibrational analysis

The experimental IR spectrum of β-C_6S_8 is shown in Fig. 7. The Raman spectrum is shown in Fig. 8. Harmonic frequencies and the corresponding intensities for both spectra were calculated at the B3LYP/cc-pVTZ level. As usual for the chosen quantum chemical model, the calculated high frequency modes systematically deviate from the experimental frequencies in the direction to higher wave numbers[36] (up to 70 cm^{-1} in the case

‡ CP corrected results of E(dimer) − ΣE(monomers) calculated at the respective crystal geometries. The BSSE amounts to 11 kJ mol^{-1} in these calculations.

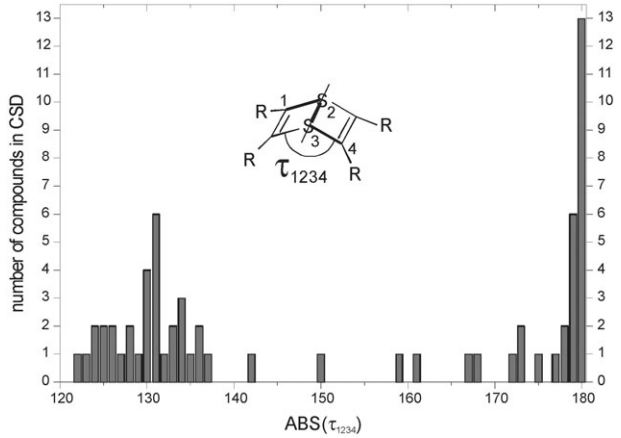

Fig. 5 Distribution of absolute dihedral angles in 66 dithiines that are found in the CSD data base (version 5.25 + 2 updates in Jan 2004). The histogram shows the number of compounds having a given τ_{1234} in one degree steps. No compounds are found with abs(τ_{1234}) < 120°.

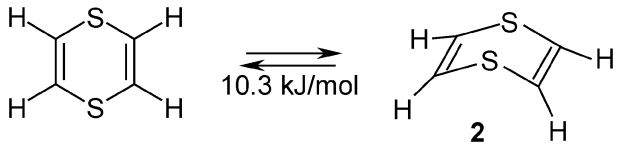

Scheme 2 1,4-Dithiacyclohexadiene in its planar and bent structure.

of ν_2). Therefore, we scaled the frequencies above 1000 cm^{-1} by an empirical scaling factor of 0.98, which was found to minimize the RMS deviation between experimental and simulated IR bands. Since the systematics of the deviation is quite obvious and as the intensity pattern of the calculated spectrum is in good agreement with the experimental one, further refinement of the theoretical data seemed unnecessary.

Table 3 gives the scaled theoretical frequencies. Simulated spectra are inserted in the corresponding Figs. 7 and 8, too. All important bands that appear in the experimental spectra can be assigned unambiguously. The assignments are noted in Table 3. The modes are labelled after their symmetry and in energetically descending order according to Herzberg's notation.[37] The characterization of the modes was made by inspection of the normal coordinate vectors, some of which are shown in Fig. 6. All 36 normal modes of the molecule are IR and Raman active, in principal. The observation of modes ν_1, ν_2, ν_{10} and

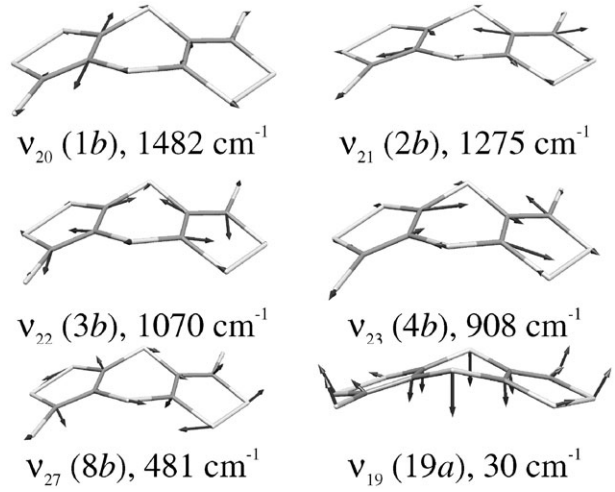

Fig. 6 Cartesian displacement vectors (arbitrary length scaling) of selected normal modes of β-C_6S_8.

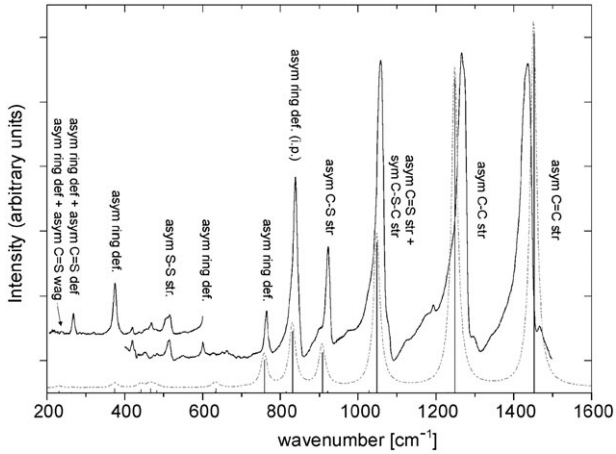

Fig. 7 Experimental (solid line) and theoretical (dashed line) IR spectrum of β-C_6S_8 (**1**). The region between 1500 and 400 cm^{-1} was measured in a KBr pellet. The upshifted part between 200 and 400 cm^{-1} was measured in a CsI pellet. The calculated line spectrum at the B3LYP/cc-pVTZ level is shown by vertical lines. Frequencies above 1000 cm^{-1} have been scaled by 0.98. The dashed line shows the calculated line spectrum convoluted with a Lorentzian lineshape function (FWHM = 20 cm^{-1}).

ν_{20} in both spectra indicates that the molecule possesses no center of inversion, which is a further indication for the non-planarity of β-C_6S_8. Due to the near-C_{2h} symmetry of the molecule a pseudo-exclusion principle holds, however, so that strong bands in the IR have only very weak—if any—counterparts in the Raman spectrum and *vice versa*.

IR spectrum. The most intense bands are of *b* symmetry, which correspond to asymmetric molecular distortions (with respect to the rotation around the C_2 axis). The intense bands at 1436, 1266, 1058 cm^{-1} can be assigned to asymmetric C=C, C–C, and C=S stretching (str) modes, respectively. The corresponding symmetric modes, which appear in a similar energetic range, show only a very weak IR activity. The band at 924 cm^{-1} in the experimental spectrum can be assigned to an asymmetric C–S str motion. Most modes below 900 cm^{-1} are ring deformation modes and show less local character. The delocalization over larger portions of the molecule makes a simple characterization difficult. We use the characterization "in plane" for motions that approximately retain the two

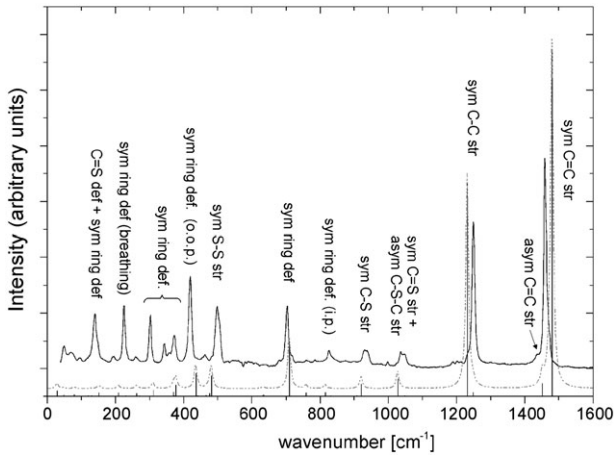

Fig. 8 Experimental (solid line) and theoretical (dashed line) Raman spectrum of β-C_6S_8 (**1**). The calculated line spectrum at the B3LYP/cc-pVTZ level is shown by vertical lines. Frequencies above 1000 cm^{-1} have been scaled by 0.98. The dashed line shows the calculated line spectrum convoluted with a Lorentzian lineshape function (FWHM = 10 cm^{-1}).

Table 3 Experimental and theoretical (B3LYP/cc-pVTZ) IR and Raman spectra of β-C_6S_8 (**1**), indicating frequencies and intensities, the symmetry and mode label following Herzberg's nomenclature and a rough characterization of the normal modes

Experiment[a]				Theory					
IR		Raman		IR		Raman		Assignment	
$\tilde{\nu}$/cm^{-1}	Int.[b]	$\tilde{\nu}$/cm^{-1}	Int.[b]	$\tilde{\nu}$/cm^{-1}[c]	Int./km mol^{-1}	Int./Å^4 amu^{-1}	Sym.	Label	Character
1467.0	vw	1457.7	vs	1480.8	0.19	488.57	A	ν_1 (1a)	Sym C=C str
1436.0	vs	1436.0	vw	1452.5	448.70	17.92	B	ν_{20} (1b)	Asym C=C str
1265.9	vs	—	—	1249.2	392.47	5.67	B	ν_{21} (2b)	Asym C–C str
1188.9	vw	1248.3	s	1231.9	0.79	299.90	A	ν_2 (2a)	Sym C–C str
1058.3	vs	—	—	1048.9	188.01	0.55	B	ν_{22} (3b)	Asym C=S str + sym C–S–C str [C(1^I)–S(3)–C(2), C(2^I)–S(3^I)–C(1) out-of-phase]
—	—	1036.9	vw	1027.9	2.91	24.22	A	ν_3 (3a)	Sym C=S str + asym C–S–C str [C(1^I)–S(3)–C(2), C(2^I)–S(3^I)–C(1) in phase]
—	—	928.3	vw	921.0	2.39	17.00	A	ν_4 (4a)	Sym C–S str [C(1^I)–S(1^I), C(1)–S(1) in phase; C(3)–S(2), C(3^I)–S(2^I) in phase]
924.0	m	—	—	908.3	50.52	0.38	B	ν_{23} (4b)	Asym C–S str [C(1^I)–S(1^I), C(1)–S(1) out-of-phase; C(3)–S(2), C(3^I)–S(2^I) out-of-phase]
840.2	s	—	—	831.6	77.42	0.33	B	ν_{24} (5b)	Asym ring def ("in plane")
—	—	827.2	vw	815.3	1.61	5.54	A	ν_5 (5a)	Sym ring def ("in plane")
764.3	w	—	—	758.9	40.85	4.68	B	ν_{25} (6b)	Asym ring def ("in plane")
—	—	707.4	w	710.0	0.84	72.06	A	ν_6 (6a)	Sym ring def + C=S def ("in plane")
601.0	vw	—	—	634.3	5.65	1.78	B	ν_{26} (7b)	Asym ring def ["out -of-plane"; on atoms C(1^I)–C(3^I)]
—	—	—	—	632.5	1.00	0.82	A	ν_7 (7a)	Sym ring def ["out of plane"; on atoms C1^I–C(3^I)]
511.0	vw	—	—	481.8	2.77	0.57	B	ν_{27} (8b)	Asym S–S str [S(2^I)–S(1^I), S(2)–S(1) out-of-phase]
—	—	506.9	w	481.8	0.02	28.87	A	ν_8 (8a)	Sym S–S str [S(2^I)–S(1^I), S(2)–S(1) in phase]
—	—	462.2	vw	476.8	0.19	4.38	A	ν_9 (9a)	Sym ring def ["out of plane"; on atoms C(1^I), C(1), C(3), C(3^I)]
468.3	vw	—	—	466.2	5.66	1.25	B	ν_{28} (9b)	Asym ring def ["out of plane"; predominantly on atoms C(1^I), C(1), C(3), C(3^I)]
455.6	vw	—		441.6	4.28	0.72	B	ν_{29} (10b)	Asym ring def [predominantly S(3), S(3^I)]
436.8	vw	430.4	m	436.3	0.64	32.05	A	ν_{10} (10a)	Sym ring def ("out of plane")
419.3	vw	—	—	409.8	0.30	0.11	B	ν_{30} (11b)	Asym ring def
—	—	386.5	vw	377.9	0.30	15.91	A	ν_{11} (11a)	Sym ring def ("rotation" of central ring)
374.4	vw	—	—	373.6	5.54	0.27	B	ν_{31} (12b)	Asym ring def ["in plane", S(2^I), S(2) move towards and away from central ring, resp.]
—	—	358.0	vw	371.0	0.06	6.13	A	ν_{12} (12a)	Sym ring def ("in plane")
321.2	vw	318.2	w	311.0	0.46	8.67	A	ν_{13} (13a)	Sym ring def ("in plane", "rotation" of outer rings)
267.5	vw	—	—	270.8	0.22	0.38	B	ν_{32} (13b)	Asym C=S def + ring def ("in plane")
—	—	243.9	w	262.6	0.54	4.24	A	ν_{14} (14a)	Sym ring def ("breathing mode")
236.1	vw	—	—	231.3	2.22	0.41	B	ν_{33} (14b)	Asym ring def + C=S wag ["out-of-plane", predominantly C(1^I)–C(3^I)]
—	—	—	—	209.5	3E–04	4.69	A	ν_{15} (15a)	Sym ring def [C(1^I)–C(3^I) in phase]
—	—	160.9	w	151.7	0.03	4.82	A	ν_{16} (16a)	Sym C=S def + sym ring def ("in plane")
—	—	—	—	147.5	2.25	0.02	B	ν_{34} (15b)	Asym ring def ("out-of-plane") + C=S def
—	—	—	—	131.2	0.16	0.04	A	ν_{17} (17a)	Sym ring def ("out-of-plane", twist of outer rings)
—	—	—	—	120.5	4.06	0.27	B	ν_{35} (16b)	Asym ring def ("out-of-plane", twist of outer rings)
—	—	—	—	79.7	0.45	1.99	B	ν_{36} (17b)	Asym C=S wag ("out of plane")
—	—	—	—	48.2	2.32	1.29	A	ν_{18} (18a)	Sym ring def ("ring torsion")
—	—	—	—	30.0	0.19	7.50	A	ν_{19} (19a)	Sym ring def ("butterfly")

[a] IR spectrum between 1600 and 500 cm^{-1} taken on a KBr pellet, IR spectrum between 500 and 200 cm^{-1} taken on a CsI pellet; Raman spectrum in the solid phase. [b] vw = very weak, w = weak, m = medium, s = strong, vs = very strong. [c] Frequencies above 1000 cm^{-1} have been scaled by an empirical scaling factor of 0.98.

planes spanned by the two C_3S_5 moieties. In contrast, the term "out-of-plane" is used when the distortion destroys the near planar conformation of the moieties. The weak band at 511 cm^{-1} in the experimental spectrum belongs to the S–S str movement. The band at 268 cm^{-1} belongs to a combination of ring in-plane and C=S deformations, whereas the band at 236 cm^{-1} can be described as an out-of-plane ring deformation plus C=S wagging mode.

Table 4 Vertical excitation energies of β-C_6S_8 to various excited states obtained from a TD-B3LYP/cc-pVTZ calculation, with the signs and the normalized weights of the leading configurations, components of the transition dipole moment (TDM) and the oscillator strength *f*

Excited state	Leading configurations[a] Sign, weight, type				Excitation energy in eV	cm^{-1}	nm	TDM[b]/e bohr *x*	*y*	*z*	*f*
Singlet states											
1^1B	(+), 45.8%, 81 → 83	(−), 27.1%, 80 → 83	(+), 16.9%, 79 → 84		2.49	20 099	498	0.0496	−0.0648	0.0000	0.0004
2^1A	(+), 36.9%, 82 → 83	(−), 31.3%, 79 → 83	(−), 12.8%, 81 → 84	(−), 11.1%, 80 → 84	2.51	20 245	494	0.0000	0.0000	0.1200	0.0009
3^1A	(+), 47.1%, 82 → 83	(+), 22.8%, 79 → 83	(+), 14.1%, 81 → 84		2.65	21 337	469	0.0000	0.0000	0.0533	0.0002
2^1B	(+), 54.2%, 82 → 84	(+), 23.0%, 81 → 83	(+), 11.2%, 80 → 83	(+), 6.0%, 82 → 86	2.87	23 183	431	0.2352	0.5173	0.0000	0.0227
3^1B	(+), 42.3%, 80 → 83	(−), 13.0%, 82 → 84	(+), 11.9%, 81 → 85	(+), 5.7%, 81 → 83	3.00	24 158	414	0.5275	−0.6377	0.0000	0.0503
4^1A	(+), 44.4%, 82 → 85	(−), 20.3%, 81 → 84	(−), 14.6%, 81 → 86		3.03	24 411	410	0.0000	0.0000	−0.027	0.0001
5^1A	(+), 27.7%, 81 → 84	(−), 27.1%, 79 → 83	(−), 19.7%, 80 → 84	(+), 11.3%, 82 → 85	3.09	24 926	401	0.0000	0.0000	0.0293	0.0001
4^1B	(+), 30.4%, 82 → 86	(−), 22.6%, 80 → 85	(+), 16.1%, 79 → 84	(−), 13.9%, 82 → 84	3.14	23 339	395	−0.1678	−0.3130	0.0000	0.0097
Triplet states											
1^3A	(+), 44.4%, 82 → 83	(−), 9.0%, 80 → 84	(−), 7.8%, 81 → 84		1.84	14 845	674	—	—	—	—
1^3B	(+), 24.2%, 82 → 84	(−), 19.8%, 80 → 83	(−), 16.3%, 81 → 83		1.91	15 378	650	—	—	—	—
2^3B	(+), 18.6%, 82 → 84	(−), 17.1%, 80 → 83	(+), 15.4%, 79 → 84		2.21	17 824	561	—	—	—	—
2^3A	(+), 27.9%, 79 → 83	(−), 14.8%, 80 → 84	(+), 7.5%, 81 → 84		2.24	18 059	554	—	—	—	—
3^3A	(+), 28.1%, 78 → 83	(+), 12.4%, 81 → 84	(+), 7.2%, 82 → 83		2.49	20 101	498	—	—	—	—
3^3B	(+), 25.8%, 82 → 84	(+), 7.0%, 81 → 83	(+), 5.6%, 78 → 84	(+), 5.3%, 80 → 83	2.63	21 231	471	—	—	—	—
3^3A	(+), 15.1%, 82 → 85	(−), 12.1%, 80 → 86	(−), 9.8%, 81 → 86	(+), 6.7%, 78 → 85	2.73	21 985	455	—	—	—	—
3^3B	(+), 13.6%, 80 → 85	(+), 10.3%, 78 → 84	(+), 9.1%, 81 → 85	(−), 8.6%, 82 → 86	2.76	22 222	450	—	—	—	—

[a] *X* → *Y* means an excitation from MO *X* to MO *Y*, see Fig. 10. [b] Components of the transition dipole moment (TDM) are calculated from the dipole length formula.

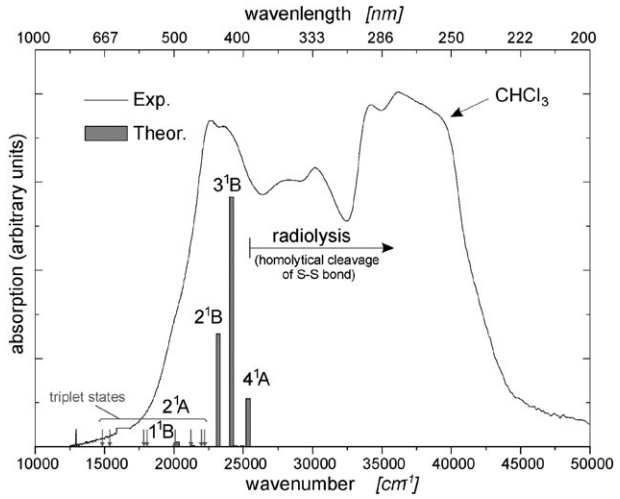

Fig. 9 UV/Vis absorption of C_6S_8: (solid line) experimental spectrum in $CHCl_3$; (vertical bars) oscillator strengths from TD-DFT calculation (B3LYP/cc-pVTZ level) for the free molecule. The location of triplet states in the low energy region is indicated by arrows. Irradiation beyond 25 000 cm^{-1} leads to decomposition.

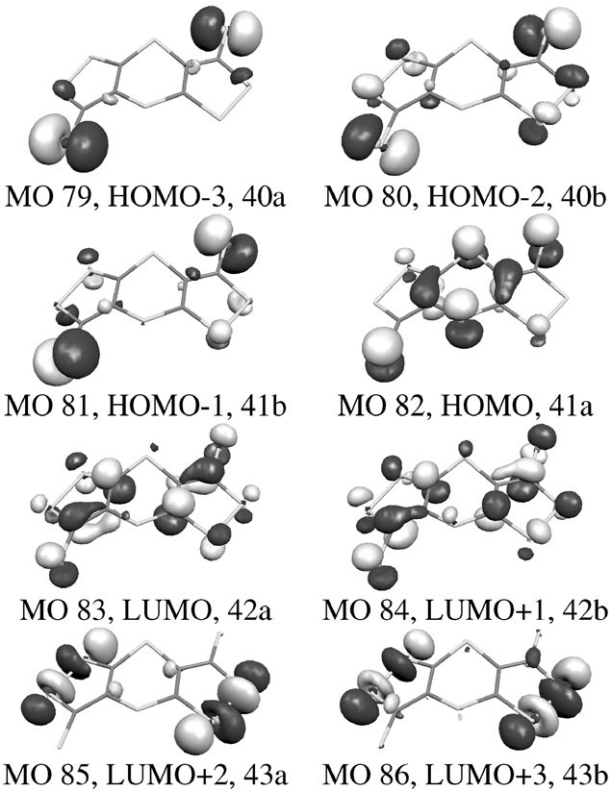

Fig. 10 Selected molecular orbitals of β-C_6S_8 (**1**) as obtained from the B3LYP/cc-pVTZ calculation.

Raman spectrum. The most intense bands at 1458 and 1248 cm^{-1} correspond to symmetric C═C str and C–C str modes, respectively. The symmetric C═S str and C–S str bands appear very weakly at 1037 and 928 cm^{-1}. Bands below 900 cm^{-1} correspond mostly to rather delocalized ring deformations, except for the band at 161 cm^{-1}, which has predominant C═S def character. We did not observe the lowest frequency mode ν_{19} (19a) experimentally. It is calculated to lie at 30 cm^{-1} (''butterfly'' motion, see Fig. 6) and corresponds to a symmetric ring deformation that induces the transition to a planar C_6S_8. The planar conformation is a transition state between two enantiomers, as shown in Fig. 4.

UV/Vis-spectrum. The experimental UV/Vis spectrum is shown in Fig. 9. Vertical excitation energies and oscillator strengths were calculated at the TD-B3LYP/cc-pVTZ level. The results are given in Table 4. The reddish color of the crystalline sample of **1** can be explained by the first two transitions to the 1^1B and 2^1A states, which absorb in the green (498 nm) and the blue (494 nm), respectively. Both transitions are dominated by nπ* excitations from non-bonding orbitals of a sulfur atom (mainly of the thione group) into the antibonding π* orbital of the S═C–C═C group (see Fig. 10). These transitions to 1^1B and 2^1A possess only a small oscillator strength. In view of several triplet states that are found in the region around 500 nm, an efficient intersystem crossing (ISC) from the singlet to the triplet manifold can be expected. Due to Kasha's rule[38] we then expect vibronic relaxation to the lowest excited triplet state. Phosphorescence from 1^3A in the region around 674 nm amplifies the color impression of red C_6S_8. In the transitions to 4^1B and 4^1A the antibonding σ-orbital of the S–S bond is populated. Hence, the cleavage of the S–S bond seems to be the first step in the decomposition of β-C_6S_8, which we observed when irradiating the compound in the UV.

Summary

The carbon sulfide C_6S_8 is dimorphic. The two crystalline forms contain molecules having a significant difference in their molecular shape. The molecule in the β-form, which is presented here for the first time, resembles the free molecule in its conformation and adopts a bent structure with a tilt angle of 133°, while the molecule in the α-form is planar. This isomerism is generally observed among differently substituted 1,4-dithiines and can be traced back to the fact that in the free molecule the transformation of the bent structure to the planar transition structure (α-form) occurs along a very flat potential, essentially the ''butterfly'' mode ν_{19} (see Fig. 6). In the crystal the large amplitude motion is likely hindered by packing effects. Also, it seems possible that packing effects in the crystal are sufficient to overcome the small energy difference and to stabilize the α-form under certain circumstances. Based on our theoretical results and our experimental observations, α-C_6S_8 is likely to be metastable. Its formation seems to be critically dependent on the conditions under which the crystal growth takes place.

To the best of our knowledge the here-presented case of C_6S_8 is the first example where this kind of isomerism is observed in a single molecule without changing the substituents or modifying the electronic situation.

Acknowledgements

The support of this work by the Deutsche Forschungsgemeinschaft within the Collaborative Research Center 408 is gratefully acknowledged.

References

1 D. D. Doxsee, C. Galloway, T. Rauchfuss, S. Wilson and X. Yang, *Inorg. Chem.*, 1993, **32**, 5467.
2 A. Ellern, J. Bernstein, J. Y. Becker, S. Zamir and L. Shalal, *Chem. Mater.*, 1994, **6**, 1378.
3 B. Ali, I. Dance, M. Scudder and D. Craig, *CrystEngComm*, 2001, 28.
4 V. S. Mastryukov, K. H. Chen, S. H. Simonsen, N. L. Allinger and J. E. Boggs, *J. Mol. Struct.*, 1997, **413**, 1.
5 G. M. Allan, R. A. Howie, J. M. S. Skakle, J. L. Wardell and S. M. S. V. Wardell, *J. Organomet. Chem.*, 2001, **627**, 189.
6 G. Steimecke, H. Sieler, R. Kirmse, W. Dietzsch and E. Hoyer, *Phosphorous, Sulfur Relat. Elem.*, 1982, **12**, 237.
7 G. M. Sheldrick, *SHELXS-93, Program for Crystal Structure Solution*, University of Göttingen, Göttingen, Germany, 1992.

8 G. M. Sheldrick, *SHELXL-93, Program for Crystal Structure Refinement*, University of Göttingen, Göttingen, Germany, 1993.
9 (*a*) A. D. Becke, *Phys. Rev. A*., 1988, **38**, 3098; (*b*) J. P. Perdew, *Phys. Rev. B*., 1986, **33**, 8822.
10 A. D. Becke, *J. Chem. Phys*., 1996, **104**, 1040.
11 (*a*) A. D. Becke, *J. Chem. Phys*., 1993, **98**, 5648; (*b*) A. Frisch and M. J. Frisch, *GAUSSIAN 98, User's Reference Guide*, Gaussian Inc., Pittsburgh, PA, USA, 1998.
12 R. Bauernschmitt and R. Ahlrichs, *Chem. Phys. Lett*., 1996, **256**, 454.
13 M. J. Frisch, G. W. Trucks, H. B. Schlegel, G. E. Scuseria, M. A. Robb, J. R. Cheeseman, V. G. Zakrzewski, J. A. Montgomery, R. E. Stratmann, J. C. Burant, S. Dapprich, J. M. Millam, A. D. Daniels, K. N. Kudin, M. C. Strain, O. Farkas, J. Tomasi, V. Barone, M. Cossi, R. Cammi, B. Mennucci, C. Pomelli, C. Adamo, S. Clifford, J. Ochterski, G. A. Petersson, P. Y. Ayala, Q. Cui, K. Morokuma, D. K. Malick, A. D. Rabuck, K. Raghavachari, J. B. Foresman, J. Cioslowski, J. V. Ortiz, B. B. Stefanov, G. Liu, A. Liashenko, P. Piskorz, I. Komaromi, R. Gomperts, R. L. Martin, D. J. Fox, T. Keith, M. A. Al-Laham, C. Y. Peng, A. Nanayakkara, C. Gonzalez, M. Challacombe, P. M. W. Gill, B. G. Johnson, W. Chen, M. W. Wong, J. L. Andres, M. Head-Gordon, E. S. Replogle and J. A. Pople, *GAUSSIAN 98*, Revision A.11, Gaussian Inc., Pittsburgh PA, 1998.
14 MOLPRO, a package of *ab initio* programs designed by H.-J. Werner and P. J. Knowles: R. D. Amos, A. Bernhardsson, A. Berning, P. Celani, D. L. Cooper, M. J. O. Deegan, A. J. Dobbyn, F. Eckert, C. Hampel, G. Hetzer, P. J. Knowles, T. Korona, R. Lindh, A. W. Lloyd, S. J. McNicholas, F. R. Manby, W. Meyer, M. E. Mura, A. Nicklaß, P. Palmieri, R. Pitzer, G. Rauhut, M. Schütz, U. Schumann, H. Stoll, A. J. S. R. Tarroni, T. Thorsteinsson and H.-J. Werner, *MOLPRO*, University of Birmingham, Birmingham, UK, 2002.
15 (*a*) J. S. Binkley, J. A. Pople and W. J. Hehre, *J. Am. Chem. Soc*., 1980, **102**, 939; (*b*) M. S. Gordon, J. S. Binkley, J. A. Pople, W. J. Pietro and W. J. Hehre, *J. Am. Chem. Soc*., 1983, **104**, 2797; (*c*) W. J. Pietro, M. M. Francl, W. J. Hehre, D. J. DeFrees, J. A. Pople and J. S. Binkley, *J. Am. Chem. Soc*., 1982, **104**, 5039.
16 T. H. Dunning, Jr., *J. Chem. Phys*., 1989, **90**, 1007.
17 (*a*) A. Schaefer, H. Horn and R. Ahlrichs, *J. Chem. Phys*., 1992, **97**, 2571; (*b*) A. Schaefer, H. Horn and R. Ahlrichs, *J. Chem. Phys*., 1994, **100**, 5829.
18 (*a*) R. A. Kendall, T. H. Dunning, Jr. and R. J. Harrison, *J. Chem. Phys*., 1992, **96**, 6769; (*b*) D. E. Woon and T. H. Dunning, Jr., *J. Chem. Phys*., 1993, **98**, 1358; (*c*) D. E. Woon and T. H. Dunning, Jr., *J. Chem. Phys*., 1995, **103**, 4572.
19 LineShaper, a f90 program for folding line spectra with lineshape functions (Gauss- or Lorentz-type): J. Weber, *LineShaper*, Universität zu Köln, Köln, Germany, 2000.
20 (*a*) P. Flükiger, H. Lüthi, S. Portmann and J. Weber, *Molekel 4.2*, Technical Report, Swiss Center for Scientific Computing, Manno, Switzerland, 2000–2002; (*b*) S. Portmann and H. P. Lüthi, *Chimia*, 2000, **54**, 766.
21 S. F. Boys and F. Bernardi, *Mol. Phys*., 1970, **19**, 553.
22 F. B. Duijneveldt, J. G. C. M. van Duijneveldt-van de Rijdt and J. H. van Lenthe, *Chem. Rev*., 1994, **94**, 1873.
23 R. Ahlrichs, M. Bär, H.-P. Baron, R. Bauernschmitt, S. Böcker, F. Furche, F. Haase, M. Häser, H. Horn, C. Hättig, C. Huber, U. Huniar, M. Kattanek, A. Köhn, C. Kölmel, M. Kollwitz, K. May, C. Ochsenfeld, H. Öhm, A. Schäfer, U. Schneider, M. Sierka, O. Treutler, B. Unterreiner, M. V. Arnim, F. Weigend, P. Weiss and H. Weiss, *TURBOMOLE v. 5*,Institut für Physikalische Chemie, Universität Karlsruhe, Karlruhe, Germany, 1998.
24 M. Feyereisen, G. Fitzgerald and A. Komornicki, *Chem. Phys. Lett*., 1993, **208**, 359.
25 F. Weigend, M. Häser, H. Patzelt and R. Ahlrichs, *Chem. Phys. Lett*., 1998, **294**, 143.
26 J. Bernstein and A. T. Hagler, *J. Am. Chem. Soc*., 1978, **100**, 673.
27 J. D. Dunitz and J. Bernstein, *Acc. Chem. Res*., 1995, **28**, 193.
28 P. Bombicz, M. Czugler, R. Tellgren and A. Kálmán, *Angew.-Chem*., 2003, **115**, 2001 (*Angew. Chem., Int. Ed*., 2003, **42**, 1957).
29 J. Weber and M. Dolg, manuscript in preparation.
30 S. Saebø, L. Radom and G. L. D. Ritchie, *J. Mol. Struct*., 1984, **108**, 59.
31 P. A. Howell, R. M. Curtis and W. N. Lipscomb, *Acta Crystallogr*., 1954, **7**, 498.
32 S. Larson, O. Simonsen, G. E. Martin, K. Smith and S. Puig-Torres, *Acta Crystallogr., Sect. C*, 1984, **40**, 103.
33 K. L. Gallaher and S. H. Bauer, *J. Chem. Soc., Faraday Trans. 2*, 1975, **71**, 1173.
34 H. Bock, A. Rauschenbach, C. Näther, M. Kleine and Z. Havlas, *Chem. Ber*., 1994, **127**, 2043.
35 A similar search was performed earlier by M. R. Bryce *et al*., who reported 43 hits of which 28 were bent and 15 planar: M. R. Bryce, A. Chesney, A. K. Lay, A. S. Batsanov and J. A. K. Howard, *J. Chem. Soc., Perkin Trans. 1*, 1999, 2451.
36 (*a*) G. Rauhut and P. Pulay, *J. Phys. Chem*., 1995, **99**, 3093; (*b*) J. A. P. Scott and L. Radom, *J. Phys. Chem*., 1996, **100**, 16502.
37 Joint Commission for Spectroscopy, *J. Chem. Phys*., 1955, **23**, 1997.
38 M. Kasha, *Discuss. Faraday Soc*., 1950, **9**, 14.